The intensification of flash droughts across China from 1981 to 2021

Shuyi Zhang (zhangsy@tea.ac.cn)
Institute of Atmospheric Physics Chinese Academy of Sciences https://orcid.org/0009-0006-5820-4681

Mingxing Li
Institute of Atmospheric Physics Chinese Academy of Sciences

Zhuguo Ma
Institute of Atmospheric Physics Chinese Academy of Sciences

Dongnan Jian
Chengdu University of Information Technology

Meixia Lv
Institute of Atmospheric Physics Chinese Academy of Sciences

Qing Yang
Institute of Atmospheric Physics Chinese Academy of Sciences

Yawen Duan
Institute of Atmospheric Physics Chinese Academy of Sciences

Doaa Amin
National Water Research Center Water Resources Research Institute

Research Article

Keywords: flash drought, soil moisture, ERA5-Land, spatiotemporal distribution, aridity index

Posted Date: June 22nd, 2023

DOI: https://doi.org/10.21203/rs.3.rs-3013606/v1

Version of Record: A version of this preprint was published at Climate Dynamics on October 3rd, 2023.
See the published version at https://doi.org/10.1007/s00382-023-06980-8.

Abstract

Flash droughts feature rapid onsets of soil moisture drought events and result in severe impacts and damages, especially on agricultural and ecological systems. How the flash drought regime across China varies on multitemporal scales with climate change is not fully clear yet. In this study, we extended the flash drought definition to apply to arid regions by adding an absolute soil moisture variation criterion. Then, we detected flash drought events across China during 1981–2021 and characterized their frequency, duration, and affected area changes on seasonal, annual, and decadal scales, using soil moisture data from the European Center for Medium-Range Weather Forecasts climate reanalysis-Land. Results show that hotspots of flash droughts appeared in North China and the Yangtze River Basin. During 1981–2021, the hotspots, even nationwide, underwent significant increases in frequencies, durations, and affected areas of flash droughts. The increases held in the extremely high values of the frequencies and durations in the decadal comparisons. Especially, North China saw the most extensive and rapid increases. Seasonally, flash drought frequencies and durations intensified more during spring and autumn, and seasonal hotspots in eastern China shifted in phase with spatial patterns of soil moisture loss balanced by precipitation and evapotranspiration. Thus, flash droughts tended to amplify atmospheric aridity. These findings on the hotspot regions and the spatiotemporal evolutions of flash droughts across China would pinpoint soil moisture responses to climate change and prepare for climate change impacts on local eco-environments.

1. Introduction

Flash drought, compared with traditional climate drought, has the characteristics of sudden occurrence, rapid development, and heavy damage, accompanied by rapid loss of soil moisture, possible high temperature, and even heat wave events (Otkin et al. 2013, 2018; Wang et al. 2016). As a result, flash drought events have massive impacts on natural environments, agriculture, ecosystem services, and the multi-aspects of society (Yuan et al. 2020). In the future, with the global temperature rising, climate drought is expected to intensify with high confidence (IPCC 2021). Droughts are projected to affect over 40% of the global population by 2030 and over 75% by 2050 (UNCCD 2022). Given the unpromising facts and projections of climate change, investigating the evolution of flash droughts, such a unique type of climate event, in response to climate change, is important. Understanding the regional impacts of climate change will supports preparedness measures for the potential risks to ecological services, grain and water supply, and socio-economic stability.

Despite the outstanding characteristics of sudden occurrence and rapid development, flash droughts are also relevant to traditional droughts both of which share some common characteristics, such as undergoing a complete process from onset to demise and developing in duration with muti-aspect impacts. In addition, flash droughts tend to subside within a sub-seasonal scale for their rapid development, while traditional droughts are focused more on slow-onset events and can last for months or years (Yuan et al. 2020). There isn't a clear boundary between the two types of droughts as they develop, and a flash drought may grow into a traditional prolonged drought (Liu et al. 2020). For this

reason, flash droughts had not been singled out as a unique type of climate droughts until the notion was proposed by Svoboda et al. (2002). In 2012, a rapidly developed drought across the Central Great Plain in the USA heavily damaged maize yield with losses of more than 30 billion US dollars (PaiMazumder and Done 2016). In the summer of 2013, a severe drought swept through the south of China in a short time, affecting 13 provinces, with more than two million hectares of crops damaged in Hunan and Guizhou provinces alone (Yuan et al. 2015). From then on, due to their huge impacts and damage in a short period, the nature of the sudden occurrence and rapid development of such drought events attracts increasing attention in climate change studies.

To distinguish flash droughts from slow-onset droughts, the conventionally used drought indices show some weakness. For example, the standardized precipitation index (SPI; McKee 1993; Mckee, Doeskin, and Kleist 1995) and the Palmer drought severity index (PDSI; Palmer 1965), with traditional time scales longer than one month, are prone to monitor long-term droughts and thus filter out the flash signals. Some vegetation-related indices show vegetation's response to drought stress, which lags behind circumstantial drought because of the hysteresis effect of vegetation physiologic processes (Otkin et al. 2013, 2014). For this reason, new criteria have been scrutinized to define flash droughts. Mo and Lettenmaier (2015) focused on representing the short-duration characteristic of a flash drought using three variables: surface air temperature deviation, evapotranspiration, and soil moisture anomalies, which is called a heat wave flash drought. Replacing soil moisture with precipitation, Mo and Lettenmaier (2016) highlighted the role played by precipitation deficit in triggering flash drought onset, also known as precipitation deficit flash droughts. To capture the rapid intensification of a flash drought, Ford and Labosier (2017) proposed an objective percentile-based method to detect the onset of a flash drought using soil moisture alone without considering the extinction of a flash drought. By improving on the percentile-based method, Yuan (2019) identified the two stages of onset and recovery based on the soil moisture variable, explicitly depicting two features of flash droughts, that is, rapid development and sustainability, and thus the complete life history of flash droughts. By now, the criteria for flash drought definition have enabled us to statistically describe the frequency, duration, and affected area of a flash drought event, establishing a foundation to investigate regional flash drought evolution in the context of changing climate.

During the past years across China, several studies have been conducted to investigate the spatiotemporal evolution of flash droughts on various scales (Yuan et al. 2015; Wang and Yuan 2018). Spatially, flash droughts are prone to emerge in wet regions in China, where the frequency and duration increase from northwest to southeast along the gradient of dry-wet climates (Yuan et al. 2019). With climate warming, flash drought frequency doubled during 1979–2010 (Wang et al. 2016). Especially, in agricultural regions flash droughts occur more frequently accompanied by heat waves and precipitation deficit mostly in spring and summer (Zhang et al. 2018). In semiarid regions, the increased intensity and duration of flash droughts are mainly associated with precipitation deficit, high temperature, and increased net radiation, with varying contributions during flash drought development (Ran et al. 2020; Fu and Wang 2022). While in humid regions, precipitation deficits dominate flash droughts (Zhang et al. 2017).

The efforts on defining a flash drought in theory and revealing spatiotemporal variability in China have formulated a paradigm for understanding flash droughts in China. Given the complexity of flash droughts, the established criteria of flash droughts, however, focus more on the flash droughts that occurred in the regions with a fair amount of surface water budgets (e.g., precipitation and evapotranspiration). Consequently, unreasonably high frequencies or long-lasting durations of flash droughts may emerge in arid and hyper-arid regions. How the non-reasonability could be filtered out from the present criteria remains open. Furthermore, the spatiotemporal dynamics of regional flash droughts based on the data with high resolution, along with their responses to the regimes of surface water budgets, are still helpful to understanding climate change impacts on terrestrial environments and ecosystems.

In this study, we focused on a criterion of flash droughts to augment and consolidate the applicability of flash drought definition across arid regions, and then we characterized the spatiotemporal evolution of flash droughts and their association with surface water budgets during 1981–2021 using a high-resolution soil moisture data set from the European Center for Medium-Range Weather Forecasts climate reanalysis-Land (ERA5-Land). The object of this study is to 1) identify hotspot regions of flash droughts across the mainland of China; 2) quantify the evolution of flash droughts during the last four decades, especially in the hotspot regions, on multiple temporal scales; 3) examine the dependency of flash drought dynamics on surface water budgets.

In the following sections, the data sets and the used methods were described, and the development on the criteria to define a flash drought was represented in Section 2. The evaluation of ERA5-Land soil moisture data, the variability of flash drought frequency, duration, and affected area, and the response of flash drought variability to surface water budgets were shown in Section 3. The possible mechanisms for flash drought variability in response to regional climate change, and implications for terrestrial environments in China, as well as the uncertainties in the present results, were discussed in Section 4. The paper was summarized with conclusions in Section 5.

2. Data and Methods

2.1. In situ observations

Soil moisture (SM) observation in China was gradually operated since 1981, there have been limited available observation data, especially the long-term continuous data in the western region. The present study used the Agrometeorological Soil Moisture Dataset (V1.0, 1981–2010, http://www.cma.gov.cn/2011qxfw/2011qsjcx), which was released by China Meteorological Administration (CMA), containing 245 in situ observation sites (geographical distribution shown in Fig. 1) over the period from 1981–2010. The monthly values were averaged from 10-day observations available at 11 layers vertically, that is, 5, 10, 20, 30, 40, 50, 60, 70, 80, 90, and 100 cm. Given the sparsity of available data during the early period and the gradual stop in 0-5cm observation data in 1994–1995, here the data for the period of 1996–2010 were used to test the reanalysis soil moisture data. In addition, the

in situ observations were temporarily suspended during frozen periods. Thus, the observations used in this study were not affected by soil freeze-thaw processes. For facilitating decision-making in agricultural practice, the soil moisture data set was released in the form of gravimetric soil moisture. With the bulk densities of soil, gravimetric soil moisture was here converted into volumetric moisture content according to formulas as follows:

$$\theta = w/\beta_w \times \beta_d$$

1

,

where, θ and w indicate volumetric and gravimetric soil moisture ($cm^3\ cm^{-3}$, $g\ g^{-1}$), respectively; β_w and β_d indicate the bulk densities of water and soil ($g\ cm^{-3}$), respectively, with β_w assumed to be 1 $g\ cm^{-3}$ normally.

2.2. ERA5-Land reanalysis data

ERA5-Land (Munoz-Sabater et al. 2021), a land surface simulation data set, was simulated with the land surface model of the European Center for Medium-Range Weather Forecasts (ECMWF, https://cds.climate.copernicus.eu/cdsapp#!/home) ERA5 climate reanalysis system, using atmospheric forcing from ERA5 reanalysis. Due to data assimilation in ERA5, ERA5-Land was influenced by observations of the atmosphere and remote sensing soil moisture only through atmospheric forcing. Compared to ERA5, this dataset provides land data with higher temporal and spatial resolutions, leading to the increased effectiveness of various complex land surface processes, such as flood or drought forecasting. The soil is resolved at 4 layers, with thicknesses of 0–7, 7–28, 28–100, and 100–289 cm, at a horizontal resolution of 0.1° × 0.1°. In this study, hourly soil volumetric moisture content at 0-100cm was used to estimate flash droughts, and monthly data of total precipitation and total evapotranspiration were used to examine the association between flash drought dynamics and surface water budgets during 1981–2021 in China.

2.3. Evaluation of ERA5-Land reanalysis data

The observation soil moisture data from 245 sites were used to test the ERA5-Land reanalysis soil moisture data during the period of 1996 to 2010 in China. Given the inconsistency between the observation depths and ERA5-Land soil layers, the observations at 10, 20, and 30 cm were averaged to compare with the reanalysis mean of the first two layers, that is, 0–7 and 7–28 cm layers. At the site scale, the comparisons of soil moisture data were conducted between observation sites and the corresponding reanalysis grids. To maximumly use the observations, we interpolated the missing values using Piecewise Cubic Hermite Interpolating Polynomial (PCHIP, David et al. 1988) once the missing values continued for more than three months, otherwise the months were excluded from comparisons. For the analysis of seasonal decomposition, the 144 sites with complete observations were used, and their mean time series was generated by averaging soil moisture data across sites along the time axis. The generated observation and reanalysis mean time series were then decomposed using the seasonal

trend decomposition based on LOESS (Local regression; Cleveland et al. 1990) in an additive model. The key method of LOESS is associated with a smoothing process based on a weighting function, in which the influence of a neighboring value on the smoothed value decreases with distance on the time axis. The rigorous mathematical deduction can be seen in the literature (Cleveland 1979; Cleveland et al. 1990). Furthermore, linear trends were acquired through the least squares linear regression method. Pearson correlation coefficients (CC) were calculated at the site scale between observation and reanalysis soil moisture data. The significance of CC was tested using the Student-T test with the degrees of freedom of $n - 2$, and the statistic t was calculated as follows:

$$r_{xy} = \frac{n\left(\sum xy\right) - \sum x \sum y}{\sqrt{\left[n\left(\sum x^2\right) - \left(\sum x\right)^2\right]\left[n\left(\sum y^2\right) - \left(\sum y\right)^2\right]]}}$$

2

,

$$t = \frac{r\sqrt{n-2}}{\sqrt{1-r^2}}$$

3

,

where x and y represent time series with sample sizes of n, and r_{xy} equals CC.

2.4. A new flash drought definition

Regarding flash droughts, in the latest Yuan's definition (Wang and Yuan 2022), both its onset and recovery processes are considered based on the pentad scale (5 days), emphasizing the rapid development and sustainability of a flash drought. More specifically, if the pentad-mean soil moisture percentile in the root zone decreases from above 40th to 20th with an average decline rate of no less than 5% in percentile per pentad, a flash drought event starts. The event ends when the soil moisture rises to above the 20th percentile with a duration of more than 4 pentads. The percentile-based constraints might mistakenly identify arid status as a long-lasting drought, especially in hyper-arid regions, leading to unreasonable implications for ecohydrological management. For this reason, based on Yuan's definition, an absolute soil moisture variation criterion was added to the established criteria, that is, soil moisture percentile dropping from 40th to 20th simultaneously with the absolute soil moisture variation larger than 0.01 $m^3\ m^{-3}$. We determined 0.01 $m^3\ m^{-3}$ as the threshold here because the magnitudes of the soil moisture seasonal variations are generally less than 0.01 $m^3\ m^{-3}$ in arid areas and our sensitivity tests showed negligible differences in flash drought identification outside arid and semiarid zones caused by the addition of the criterion. The determination of the onset, duration, and end of a flash drought is schematically illustrated in Fig. 2 with this added criterion.

2.5. Statistical analysis

To statistically describe the spatiotemporal characteristics of flash droughts in China during 1981–2021, the frequency of flash droughts was determined as the total number of onsets on each grid during the study period. The total duration refers to the pentads between the onset and end of a flash drought, and the mean duration is a division of the total duration by the frequency. To compare the affected areas across various climate zones, an area index was defined as the ratio of the number of grids that experienced flash droughts to the total grid number in a study area or climate zones. Furthermore, based on the mean annual precipitation total from 1981 to 2021, we divided the study area into four dry-wet climate zones. Regions with annual precipitation less than 200mm, 200-400mm, 400-800mm, and greater than 800 mm were classified into arid, semiarid, subhumid, and humid zones, respectively (Fig. 1). To put the flash drought variability in the dry-wet context of climate, the aridity index (AI) of potential evapotranspiration to precipitation was used to represent the climatic dryness.

2.6. Partial correlation analysis

To quantify the relationship between flash drought occurrence and terrestrial water balances, a partial correlation analysis was conducted on a monthly scale. Partial correlation coefficients (PCC) of flash drought frequencies concerning precipitation (Pr) and evapotranspiration (ET) anomalies were calculated separately using the 41-year monthly mean frequencies and monthly anomalies of Pr and ET for all grid points. The means of climate zones were derived by averaging across grids within each climate zone with the weights of grid areas. Seasonal coefficients were computed using the averaged data of each season during the 41 years. The significance of PCC was tested using the Student-T test with the degrees of freedom of $n - k - 2$, and the statistic t was calculated as follows:

$$r_{xy \bullet z} = \frac{r_{xy} - r_{xz} r_{yz}}{\sqrt{\left(1 - r_{xz}^2\right)\left(1 - r_{yz}^2\right)}}$$

4

,

$$t = \frac{r\sqrt{n - k - 2}}{\sqrt{1 - r^2}}$$

5

,

where r_{xy}, r_{xz}, and r_{yz} represent CCs between the x, y, and z time series. n is the sample size, k is the number of controlled variable, and $r_{xy \bullet z}$ equals PCC.

3. Results

3.1. Evaluation of ERA5-Land soil moisture data

The ERA5-Land reanalysis soil moisture data, used to examine flash droughts, was evaluated against in situ observations in 1996–2010. At the site scale, significant CCs between observations and reanalysis data were distributed extensively with reasonable spatial representativeness (Fig. 3a). There were 163 (170) of 182 sites passed the significance test with a confidence level of 99% (95%), accounting for 89.56% (93.40%). The low CCs were mainly located in Northeast China, Inner Mongolia, Xinjiang, and the Tibet Plateau, largely associated with the complex topography. Given the inevitable biases due to the inconsistent depths of observation and reanalysis data (Sec. 2.1, 2.2), both the site-averaged value of 0.08 $m^3 m^{-3}$ for root mean square errors and spatial uniformity of mean absolute errors indicated reasonable fidelity of reanalysis soil moisture data across China (Fig. 3b). Considering the mismatch of spatial representativeness between observation sites and model grids, the site-averaged time series weregenerated (Sec. 2.3) to reduce the effects from individual sites and then the analysis of seasonal decomposition was conducted (Fig. 4). For the site-averaged time series, CC between the site-averaged time series of observations and reanalysis soil moisture data reached 0.73 (Fig. 4a), suggesting the enhanced inconsistent depths of observation and reanalysis data (Sec. 2.1, 2.2), both the site-averaged value of 0.08 $m^3 m^{-3}$ for root mean square errors and spatial uniformity of mean absolute errors indicated reasonable fidelity of reanalysis soil moisture data across China (Fig. 3b). Considering the mismatch of spatial representativeness between observation sites and model grids, the site-averaged time series were generated (Sec. 2.3) to reduce the effects from individual sites and then the analysis of seasonal decomposition was conducted (Fig. 4). For the site-averaged time series, CC between the site-averaged time series of observations and reanalysis soil moisture data reached 0.73 (Fig. 4a), suggesting the enhanced reasonability of ERA5-Land soil moisture data on a regional scale across China. The trend terms show that the reanalysis data performed well in generating observed low-frequency variability of soil moisture with a CC of 0.80 (Fig. 4b). The linear trends were − 0.03 $m^3 m^{-3}$ and − 0.01 $m^3 m^{-3}$ during 1996–2010 ($P < 0.01$) for the reanalysis and observations data, respectively, and the reanalysis data captured the observed decrease during 1996–2010 despite much faster trend. Regarding seasonal terms, the reanalysis data largely regenerated the observed seasonal dynamics, although there was a substantial bias in seasonal spread (Fig. 4c). The correlation of residual terms reached 0.86 (Fig. 4d) indicating high fidelity of monthly dynamics in the reanalysis soil moisture data during 1996–2010. In general, ERA5-Land reanalysis soil moisture data reasonably agreed with the observations, grasping the main characteristics of variations on multiple scales in China, despite the insufficient evaluations here on absolute magnitudes due to the unavailability of the soil moisture observations layer that fully match the model soil layer depths. In this regard, the recent studies have evaluated the terrestrial water cycle components as well as relevant energy balances on various spatiotemporal scales (Li et al. 2020, 2022; Wu et al. 2021)not only to demonstrate the adequacy of water variable magnitudes but also to model physical process representations. Furthermore, the uncertainties in the reanalysis soil moisture data and its effects on the results were discussed in Section 4.

3.2. Spatial characteristics of flash droughts

Flash drought events occurred in a wide range of regions in China during 1981–2021 (Fig. 5a).The hotspot regions concentrated in the semiarid Northwest and North China and the humid Yangtze River Basin. The frequency reached 17 and 21 times per decade in the two regions, respectively. From a perspective of topography, the mountainous regions were prone to see high-frequency flash droughts, largely associated with quicker water balances and higher wind speeds forced by topography (Yeh and Eltahir 1998; Yoo and Kim 2004; Su et al. 2018; Chen et al. 2022). While regions with the low frequency of flash droughts lay in high latitudes and altitudes, where soil moisture variations were restrained as the soil is frozen. In most hyper-arid regions, such as the extensive deserts in the Northwest and the west of the Tibetan Plateau, the flash droughts were determined as less than 5 events per decade due to long dry status and less and short fluctuations in soil moisture. Regarding the spatial pattern of flash drought durations (Fig. 5b), it was characterized by a tri-pole distribution, that is, long in the north and south and short in the central. The long poles lay in Northeast and South China, respectively, with durations of 12–16 pentads; the short pole was centered from the Yellow River and Yangtze River basins with durations of 8–10 pentads. In addition, in peripheral areas of the Tibetan Plateau, there appeared flash droughts lasting 14–18 pentads. In parts of the hotspot regions with high frequencies, the durations were also long, suggesting frequent and lasting impacts of flash droughts. Overall, in the past 41 years, an average of 11 events in a decade and 11 pentads in the duration of flash drought events occurred on the grid points in the study area. The spatial patterns of frequency and duration show upward trends in most parts of China (Fig. 5c, d). In particular, the North China hotspot regions underwent significantly intensified flash droughts in terms of both frequency and duration. The same trends held in semiarid Northwest China and regions from the Yangtze-Han River to the Yangtze-Huaihe River basins. The linear trends ranged from 0.3–0.5 times per decade for frequency and 0.3–0.8 pentads per time per year for the duration in the regions with significant trends during 1981–2021. In contrast, significant downward trends in frequency and duration were observed in the peripheral regions of the Tibetan Plateau and parts of the arid zone, with maximum trends reaching − 0.4 times per decade and − 0.5 pentads per time per year, respectively.

3.3. Temporal characteristics of flash droughts

3.3.1. Interannual and decadal variabilities

On the interannual scale, the three characteristics of flash droughts, that is, frequency, duration, and affected area ratio, show upward linear trends across four climate zones during 1981–2021 (Fig. 6). The frequencies increased with the highest frequency of 1.25 times per year in the humid zone, followed by 1.1 times per year in subhumid and semiarid zones, the lowest frequency of 0.86 times per year in the arid zone, on average. In terms of total duration, the average increase was the fastest in the subhumid zone with a rate of 0.2 pentads per year, followed by 0.13 in the arid zone. However, the increasing rates in humid and semiarid zones were not significant. As for the affected area ratio over 1981–2021, 83.34% of the humid zone was affected by flash drought events, followed by approximately 70% in subhumid and semiarid zones, and 46.60% in arid areas. Among the climate zones, the growing trend was the

highest in the subhumid zone reaching a rate of 0.69% per year, and the rates for the other three areas ranged from 0.2–0.35% per year. On the top of interannual dynamics and linear trends, there were longer fluctuations in flash drought evolution in 1981–2021. Notably, from 2000 to 2007, the intensification in flash droughts across four climate zones was occurred, consistent with the a reduction in precipitation, surface water resources, and vegetation index in China on average (CMA Climate Change Centre 2021), which contributed to the significant downward trends in flash droughts, especially after 2007 in arid zones (Fig. 5c, d, Fig. 6). Furthermore, across four climate zones, the proportional variations of the three characteristic variables weighted with grid areas show that humid and subhumid zones contribute largely to China's flash droughts (Fig. 7 with statistics in Table 1). Three characteristic variables underwent rapid growths since 2000 reaching their maximums in 2007, and this amplitude of the increase in decadal mean in the 2000s gradually grew from humid areas to arid areas (Fig. 6) indicating that arid zone was mostly sensitive to the long-lasting climate fluctuations. On the decadal scale, the probability distributions for the four decades (Fig. 8) illustrated that flash drought frequencies and durations were overall increased, in terms of both mean and extremely high values, from the 1980s to 2010s. Specifically, flash droughts were growing to be more frequent and long-lasting with climate change across China, although there were, to varying extents, mitigation during the 2010s relative to the 2000s. By contrast, the probability density functions of the surface atmospheric aridity index (Fig. 8i-l) show a slight increase in dryness. Such a discrepancy indicates a disproportionate association between atmospheric and soil aridity changes, and that the soil tends to amplify the atmospheric dry anomalies forced by land-atmosphere feedback with climate change over the past 41 years.

Table 1
The proportion of four climate zones to the annual frequency, total duration, and affected area of flash droughts in China from 1981–2021

Variables\Zones	Humid	Subhumid	Semiarid	Arid
Freq	45.33%	34.70%	13.16%	6.81%
Dur	42.79%	36.04%	13.57%	7.59%
Area	46.09%	36.41%	11.87%	5.63%

3.3.2. Seasonal variability

As for seasonality of flash drought dynamics, there were remarkable spatial shifts in seasonal hotspot regions in China during 1981–2021 (Fig. 9). From spring to autumn, flash droughts occurred most frequently in North China, then the Yangtze River basin, and then South China, with the maximum frequency approximately 10 times per decade and lasting 7 pentads. In winter, flash droughts occurred with relatively high frequencies of 5–6 times per decade in parts of Southwest China. In terms of duration, the seasonal hotspot regions were more extensive despite the analogous spatial patterns. Such spatial shifts in seasonal hotspot regions were largely in phase with the movement of solar radiation and precipitation belts with summer monsoon in Eastern China (He et al. 2007). In terms of trend seasonality,

the hotspot regions in North China, the Yangtze-Han River, and Yangtze-Huai River basins experienced significant intensification during all seasons, according to both frequency and duration. Especially in North China, the maximum increasing trends reached 0.4 times per decade in frequency and 0.25 pentads per year in duration. However, in northern North China and peripheral regions of the Tibetan Plateau, downward trends appeared during various seasons. From the perspective of annual cycles of climate zone-averaged characteristic variables (Fig. 10), in the humid zone, flash droughts show three peak frequencies in April, July, and October, reaching 1.10, 1.79, and 1.75 times per decade. The responding durations and affected areas kept rising from February to October or even later, with a maximum duration of 15.33 pentads per decade and 79.38% of humid areas. In subhumid and semiarid zones, the peak frequencies of 2.52/2.26 times per decade appeared in May with the peak of durations and affected areas appearing in the next month, June, reaching 18.66/16.78 pentads per decade and 93.32%/89.67% of the zone areas, respectively, followed by sub-large values in autumn. In the arid zone, the annual cycles of the three variables show a similar mode as those of the subhumid and semiarid zones, but with lower peak values (1.38 times per decade, 12.55 pentads per decade, and 74.08%, respectively). For interdecadal evolutions, these three characteristic variables generally peaked in the spring or autumn of a year.

3.4. Flash droughts response to surface water balance

To quantify flash drought response to surface water balances, a partial correlation analysis was conducted between flash drought frequencies and Pr and ET variations for the period of 1981–2021 (Fig. 11). Overall, flash drought frequencies were positively correlated with ET anomalies and negatively correlated with Pr anomalies, suggesting that Pr deficit and ET excess lead to flash drought onset and quick development. Notably, the two flash drought hotspot regions, that is, North China and the Yangtze River Basin, show significant correlations with both Pr and ET anomalies. However, the Pr deficit played a leading role in North China, while it was ET excess that dominated flash drought frequencies in the Yangtze River Basin. Additionally, in Northwest China, both positive correlations with Pr and ET anomalies reveal that flash drought frequencies were determined by the ET excesses over the increases of Pr in arid and semiarid regions. In contrast, negative correlations indicate that decreased Pr leads to declined ET and the more frequent onset of flash droughts in the Northwest and Southwest regions. Furthermore, across climate zones, the monthly dynamics of partial correlations (Fig. 12) show that the significant correlations of flash drought frequencies with Pr and ET anomalies occurred in various months of spring, summer, and autumn. The changes in magnitudes of coefficients, and even their signs, suggest that flash drought evolutions with soil moisture gain and loss processes could be observed on a monthly scale, representing the regime changes of surface water and solar radiation balances by the way of Pr and ET anomalies across various climate zones. Specifically, for the shifts of seasonal hotspot regions (Fig. 13), the negative correlation with Pr and the positive with ET suggests that Pr deficits and ET increases contributed to frequent flash droughts in North China in spring. In the Yangtze River Basin, positive correlations with both Pr and ET indicate that more rapid increases in ET over Pr in summer led to increases of flash drought events in summer. In autumn, negative correlations with both Pr and ET in

parts of South China suggest Pr deficits led to both decreases in ET and increases in flash drought eventsin these regions.

4. Discussion

4.1. Development in flash drought definition

Our new addition of flash drought criteria highlighted the vegetation's perception of rapidly changing water stress during a flash drought. The threshold of absolute variations (over 0.01 m^3 m^{-3}) allowed for the filtering out of slight fluctuations in soil moisture content despite large percentile spans especially in hyper-arid regions, meanwhile, to detect the vegetation perceptible water losses in the soil across arid and semiarid regions, for instance, parts of the Tibet Plateau and arid-semiarid Northwest China (Fig. 5, 14). In addition, the thresholds of soil moisture were determined according to land cover classification and vegetation-targeted sensitivity testing, with which various thresholds featuring diverse magnitudes, regions, and periods could be explored in future studies (Ford and Labosier 2017). Furthermore, our study focused on year-round flash drought changes rather than during the growing seasons. The seasonal hotspot regions of flash droughts shifted from North China to the Yangtze River Basin and their responses to Pr and ET balances further helped to dissect mechanisms and ecological effects of flash drought evolution. Based on the established and added criteria, hotspot regions of flash droughts overall followed the Pr gradient in China, agreeing with that of existing research (Yuan et al. 2019; Christian et al. 2021; Wang and Yuan 2022; Fu and Wang 2022). However, the newly added criterion of flash drought detection as well as the high horizontal resolution of ERA5-Land soil moisture data largely contributed to the hotspot regions in North China and mountainous regions.

4.2. Possible mechanisms for flash drought changes in different climate zones

The present study found that flash droughts occurred when Pr and ET concurrently increased (positive correlations) in the growing seasons in humid regions. Previous studies have shown that, during growingseason of humid climate, rapid increases in evaporation demand with high temperature, strong wind, and strong solar radiation, exceed Pr and thus quickly deplete soil moisture in the root zone (Otkin et al. 2013, 2016; Mo and Lettenmaier 2015). As a result, the quick depletion of soil moisture triggers the onset of flash droughts. In this regard, the transition of soil moisture losses from energy-limited to water-limited may play an indicative role in flash drought monitoring (Hunt et al. 2009, 2014; Ford et al. 2015). In addition, vegetation by drawing more water from the deeper soil layers during a drought further exacerbates soil moisture deficit and the flash drought onset, which in turn leads to vegetation damage (Wang et al. 2016). In arid regions, the ET amount is regulated by available moisture rather than solar radiation energy. During the past decades, Northwest China experienced a warming-wetting change in climate (Ma and Fu 2001), which alleviated the moisture deficit and even generated decreases in flash drought frequencies in parts of these regions. However, the intensified ET with rising surface air

temperature leads to more rapid losses of soil moisture, which is responsible for the overall upward trends of flash drought frequency in arid regions (Fig. 6). Regarding the seasonal shifts in flash drought hotspots from North China to the Yangtze River Basin, they overall align with the moving rainfall belt in eastern China under the control of the advance and retreat of the East Asian summer monsoon (EASM) and the western Pacific subtropical high (WPSH; Chen et al. 2006). In spring, the rainfall belt lies in South China, while in North China, the rapidly increased ET due to the rising air temperature, wind speed, and solar radiation, depletes soil moisture and thus increases the frequencies (Otkin et al. 2013; Mo and Lettenmaier 2015). In summer, the summer monsoon belt moves northward after the Meiyu season, and WPSH controls the middle and lower Yangtze River Basin. Thus, ET rapidly depletes Pr and soil moisture and promotes flash drought occurrence. In autumn, with EASM retreating out of South China, WPSH again affects the Yangtze River Basin and its southern regions, which is responsible for the southward expansion of flash drought hotspot regions. Although the annual frequency of flash droughts is significantly correlated with Pr and ET, Pr deficit determines the onset of flash droughts with a ratio of 92%, and ET excess largely regulates the speed of onset through land-atmosphere coupling (Wang and Yuan 2022). Furthermore, during past decades, with rising air temperatures and declining intensity of EASM, decreased rainfall in North China has been observed since the mid-1960s leading to intensifying frequent flash droughts in this region (Zhang 2015; Chen et al. 2021). Meanwhile, the weakening EASM, accompanied by the westward extension of the WPSH, promotes the westward transport of water vapor from the Indian Ocean and the Pacific that contributes to the increases in Pr in Northwest China, leading to downward trends in flash drought frequencies in the region (Chen et al. 2021).

4.3. Limitations, uncertainty, and outlook

This study mainly focused on the spatiotemporal characteristics of flash drought and their associations with terrestrial water balances using ERA5-Land reanalysis data. The reanalysis soil moisture data is, to varying extents, inconsistent with observations across China, especially in long-term trends (Fig. 4). The trend biases might lead to an enlarged intensification in flash drought frequencies, durations, and affected areas. The model systems of ERA5-Land reanalysis have yet to incorporate representations of human activities such as agricultural irrigation, water resource management, and ecological engineering, which might contribute to flash drought detection biases on a local scale. It is, however, worth noting that the in situ observations of soil moisture data might not completely represent the mean status of a model grid. As flash drought is still a newly emerging concept in climate study, to apply to regions with dry climates, in this study a criterion of the absolute amount of soil moisture was set by the sensitive testing method. The criterion suggests a direction to detect flash droughts by considering ecological effects that can act as a reference to other regions, but its region-specific applicability required further testing based on the ecohydrological indicators. In the future, thorough thinking of the flash drought criteria is necessary to facilitate practical monitoring, forecasting, and early warning. Finally, the synoptic and climatic mechanisms for flash drought change, especially for its responses to warming climate, are fundamentally important.

5. Summary and conclusions

In this study, from the perspective of spatiotemporal evolution, flash droughts have been examined across China under changing climate from 1981 to 2021, using ERA5-Land reanalysis soil moisture data. Furthermore, how flash droughts respond to surface water and solar radiation balances with climate change has also been investigated, based on the partial association of flash droughts with precipitation and evapotranspiration variations. The main conclusions were drawn as follows.

1) Flash drought hotspot regions were mainly located in North China and the Yangtze River Basin, while long-lasting flash drought events were prone to appear in Northeast and South China. In addition, the mountainous regions were prone to see high-frequency flash droughts.

2) With climate change, the frequency and duration presented consistent upward trends in the hotspot regions during 1981–2021. Notably, in North China, Northwest China, and the Yangtze-Han River to the Yangtze-Huaihe River basins, upward trends were significant. In contrast, decreasing trends were observed in the peripheral regions of the Tibetan Plateau and parts of the arid zone. The overall changes tended to intensify both in means and extremes across four climate zones.

3) Flash droughts prevailed from spring to autumn. Hotspot regions emerging from North China to the Yangtze River Basin to South China in turn were changeably dominated by soil moisture gain and loss processes, which were driven by the regime of surface water and solar radiation balances across various climate zones.

This study has added further evidence based on the reanalysis soil moisture data that such a specific type of drought, flash drought, intensified in China during the past 41 years. With climate change, the regime of surface water and solar radiation balances was largely associated with the reported flash drought intensification. These findings suggested that on top of the dry-wet seasonality of climate across China, droughts of flash onset, rapid development, and lengthening duration has been increasingly characterized the climate change impacts on terrestrial ecohydrological systems. Thus, the far-reaching impacts of flash droughts on terrestrial ecosystem services, food security, and water resources deserve further studies in the future.

Declarations

Funding This work was jointly supported by the National Natural Science Foundation of China (42075171, 42130613), the scientific research fund of Chengdu University of Information Technology (KYTZ202122).

Conflict of interest There is no conflict of interest between the authors.

Author contributions Material preparation and analysis were performed by Shuyi Zhang, data collection was performed by Dongnan Jian, and the manuscript was written by Mingxing Li and Shuyi Zhang. All authors commented on previous versions of the manuscript.

Data availability The ERA5-Land reanalysis data are obtained from https://cds.climate.copernicus.eu/cdsapp#!/home, and the Agrometeorological Soil Moisture Dataset is available at http://www.cma.gov.cn/2011qxfw/2011qsjcx.

References

1. Chen F, Chen J, Huang W (2021) Weakened East Asian summer monsoon triggers increased precipitation in Northwest China. Sci China Earth Sci 64:835–837. https://doi.org/10.1007/s11430-020-9731-7
2. Chen H, Wang C, Meng X, et al (2022) Triggering Mechanism of Extreme Wind over the Complex Mountain Area in Dali Region on the Yunnan-Guizhou Plateau, China. Atmosphere 13:133. https://doi.org/10.3390/atmos13010133
3. Chen L, Zhang B, Zhang Y (2006) Progress in Research on the East Asian Monsoon. J Appl Meteor Sci 17:711–724. https://doi.org/10.11898/1001-7313.20060609
4. Christian JI, Basara JB, Hunt ED, et al (2021) Global distribution, trends, and drivers of flash drought occurrence. Nat Commun 12:6330. https://doi.org/10.1038/s41467-021-26692-z
5. Cleveland RB, Cleveland WS, McRae JE, Terpenning I (1990) STL: A Seasonal-Trend Decomposition Procedure Based on Loess. J Off Stat 6:3–33. https://www.scb.se/contentassets/ca21efb41fee47d293bbee295bf297be297fb293/stl-a-seasonal-trend-decomposition-procedure-based-on-loess.pdf
6. Cleveland WS (1979) Robust Locally Weighted Regression and Smoothing Scatterplots. J Am Stat Assoc 74:892–836.http://links.jstor.org/sici?sici=0162-1459%28197912%2974%3A368%3C829%3ARLWRAS%3E2.0.CO%3B2-L
7. CMA Climate Change Centre (2021) Blue Book on Climate Change in China. Science Press, Beijing
8. David K, Cleve M, Stephen N (1988) Numerical Methods and Software. Prentice Hall, New Jersey, United States
9. Ford TW, Labosier CF (2017) Meteorological conditions associated with the onset of flash drought in the Eastern United States. Agric For Meteorol 247:414–423. http://dx.doi.org/10.1016/j.agrformet.2017.08.031
10. Ford TW, McRoberts DB, Quiring SM, Hall RE (2015) On the utility of in situ soil moisture observations for flash drought early warning in Oklahoma, USA. Geophys Res Lett 42:9790–9798. https://doi.org/10.1002/2015GL066600
11. Fu K, Wang K (2022) Quantifying Flash Droughts Over China From 1980 to 2017. J Geophys Res Atmos 127:e2022JD037152. https://doi.org/10.1029/2022JD037152
12. He J, Ju J, Wen Z, et al (2007) A review of recent advances in research on Asian monsoon in China. Adv Atmos Sci 24:972–992. https://doi.org/10.1007/s00376-007-0972-2
13. Hunt ED, Hubbard KG, Wilhite DA, et al (2009) The development and evaluation of a soil moisture index. Int J Climatol 29:747–759. https://doi.org/10.1002/joc.1749

14. Hunt ED, Svoboda M, Wardlow B, et al (2014) Monitoring the effects of rapid onset of drought on non-irrigated maize with agronomic data and climate-based drought indices. Agric For Meteorol 191:1–11. http://dx.doi.org/10.1016/j.agrformet.2014.02.001
15. IPCC (2021) Climate Change 2021: The Physical Science Basis. Contribution of Working Group I to the Sixth Assessment Report of the Intergovernmental Panel on Climate Change. Cambridge University Press, Cambridge, United Kingdom and New York, NY, USA
16. Li M, Ma Z, Wu P, et al (2022) Ecological Response to Climate Change Across China From Combined Soil Temperature and Moisture Changes. Earth Space Sci 9:e2022EA002640. https://doi.org/10.1029/2022EA002640
17. Li M, Wu P, Ma Z (2020) A comprehensive evaluation of soil moisture and soil temperature from third-generation atmospheric and land reanalysis data sets. Int J Climatol 40:5744–5766. https://doi.org/10.1002/joc.6549
18. Liu Y, Zhu Y, Zhang L, et al (2020) Flash droughts characterization over China: From a perspective of the rapid intensification rate. Sci Total Environ 704:135373. https://doi.org/10.1016/j.scitotenv.2019.135373
19. Ma Z, Fu C (2001) Trend of surface humid index in the arid area of northern China. Acta Meteorol Sin 6:737–746. https://doi.org/10.11676/qxxb2001.077
20. McKee TB, Doesken NJ, Kleist J (1993) The relationship of drought frequency and duration to time scales. In: 8th Conference on Applied Climatology. American Meteorological Society, Anaheim, California, pp 179–183
21. Mckee TB, Doeskin NJ, Kleist J (1995) Drought Monitoring With Multiple Time Scales. In: 9th Conference on Applied Climatology. American Meteorological Society, Dallas, Texas, pp 233–236
22. Mo KC, Lettenmaier DP (2015) Heat wave flash droughts in decline. Geophys Res Lett 42:2823–2829. https://doi.org/10.1002/2015GL064018
23. Mo KC, Lettenmaier DP (2016) Precipitation Deficit Flash Droughts over the United States. J Hydrometeorol 17:1169–1184. https://doi.org/10.1175/JHM-D-15-0158.1
24. Munoz-Sabater J, Dutra E, Agusti-Panareda A, et al (2021) ERA5-Land: a state-of-the-art global reanalysis dataset for land applications. Earth Syst Sci Data 13:4349–4383. https://doi.org/10.5194/essd-13-4349-2021
25. Otkin JA, Anderson MC, Hain C, et al (2013) Examining Rapid Onset Drought Development Using the Thermal Infrared-Based Evaporative Stress Index. J Hydrometeorol 14:1057–1074. https://doi.org/10.1175/JHM-D-12-0144.1
26. Otkin JA, Anderson MC, Hain C, et al (2016) Assessing the evolution of soil moisture and vegetation conditions during the 2012 United States flash drought. Agric For Meteorol 218:230–242. http://dx.doi.org/10.1016/j.agrformet.2015.12.065
27. Otkin JA, Anderson MC, Hain C, Svoboda M (2014) Examining the Relationship between Drought Development and Rapid Changes in the Evaporative Stress Index. J Hydrometeorol 15:938–956. https://doi.org/10.1175/JHM-D-13-0110.1

28. Otkin JA, Svoboda M, Hunt ED, et al (2018) FLASH DROUGHTS A Review and Assessment of the Challenges Imposed by Rapid-Onset Droughts in the United States. Bull Amer Meteorol Soc 99:911–919. https://doi.org/10.1175/BAMS-D-17-0149.1
29. PaiMazumder D, Done JM (2016) Potential predictability sources of the 2012 US drought in observations and a regional model ensemble. J Geophys Res Atmos 121:12581–12592. https://doi.org/10.1002/2016JD025322
30. Palmer WC (1965) Meteorological Drought. In: Weather Bureau. U.S. Department of Commerce, Washington, DC, p 58
31. Ran H, Li J, Zhou Z, et al (2020) Predicting the spatiotemporal characteristics of flash droughts with downscaled CMIP5 models in the Jinghe River basin of China. Environ Sci Pollut Res 27:40370–40382. https://doi.org/10.1007/s11356-020-10036-3
32. Su T, Li Z, Kahn R (2018) Relationships between the planetary boundary layer height and surface pollutants derived from lidar observations over China: regional pattern and influencing factors. Atmos Chem Phys 18:15921–15935. https://doi.org/10.5194/acp-18-15921-2018
33. Svoboda M, LeComte D, Hayes M, et al (2002) The drought monitor. Bull Amer Meteorol Soc 83:1181–1190. https://doi.org/10.1175/1520-0477-83.8.1181
34. UNCCD (2022) Drought in numbers 2022. UNCCD, Madrid, Spain
35. Wang L, Yuan X (2018) Two Types of Flash Drought and Their Connections with Seasonal Drought. Adv Atmos Sci 35:1478–1490. https://doi.org/10.1007/s00376-018-8047-0
36. Wang L, Yuan X, Xie Z, et al (2016) Increasing flash droughts over China during the recent global warming hiatus. Sci Rep 6:30571. https://doi.org/10.1038/srep30571
37. Wang Y, Yuan X (2022) Land-atmosphere coupling speeds up flash drought onset. Sci Total Environ 851:158109. https://doi.org/10.1016/j.scitotenv.2022.158109
38. Wu Z, Feng H, He H, et al (2021) Evaluation of Soil Moisture Climatology and Anomaly Components Derived From ERA5-Land and GLDAS-2.1 in China. Water Resour Manag 35:629–643. https://doi.org/10.1007/s11269-020-02743-w
39. Yeh PJF, Eltahir EAB (1998) Stochastic analysis of the relationship between topography and the spatial distribution of soil moisture. Water Resour Res 34:1251–1263. https://doi.org/10.1029/98WR00093
40. Yoo C, Kim S (2004) EOF analysis of surface soil moisture field variability. Adv Water Resour 27:831–842. https://doi.org/10.1016/j.advwatres.2004.04.003
41. Yuan X, Ma Z, Pan M, Shi C (2015) Microwave remote sensing of short-term droughts during crop growing seasons. Geophys Res Lett 42:4394–4401. https://doi.org/10.1002/2015GL064125
42. Yuan X, Wang L, Wu P, et al (2019) Anthropogenic shift towards higher risk of flash drought over China. Nat Commun 10:4661. https://doi.org/10.1038/s41467-019-12692-7
43. Yuan X, Wang W, Zhang M, Wang L (2020) A few thoughts on the study of flash drought. Trans Atmos Sci 43:225–237. https://doi.org/10.13878/j.cnki.dqkxxb.20191105005

44. Zhang R (2015) Changes in East Asian summer monsoon and summer rainfall over eastern China during recent decades. Sci Bull 60:1222–1224. https://doi.org/10.1007/s11434-015-0824-x
45. Zhang X, Chen N, Hu C, Peng X (2018) Spatio-temporal Distribution of Three Kinds of Flash Droughts over Agricultural Land in China from 1983 to 2015. Adv Earth Sci 33:1048–1057. https://doi.org/10.11867/j.issn.1001-8166.2018.10.1048.
46. Zhang Y, You Q, Chen C, Li X (2017) Flash droughts in a typical humid and subtropical basin: A case study in the Gan River Basin, China. J Hydrol 551:162–176. https://doi.org/10.1016/j.jhydrol.2017.05.044

Figures

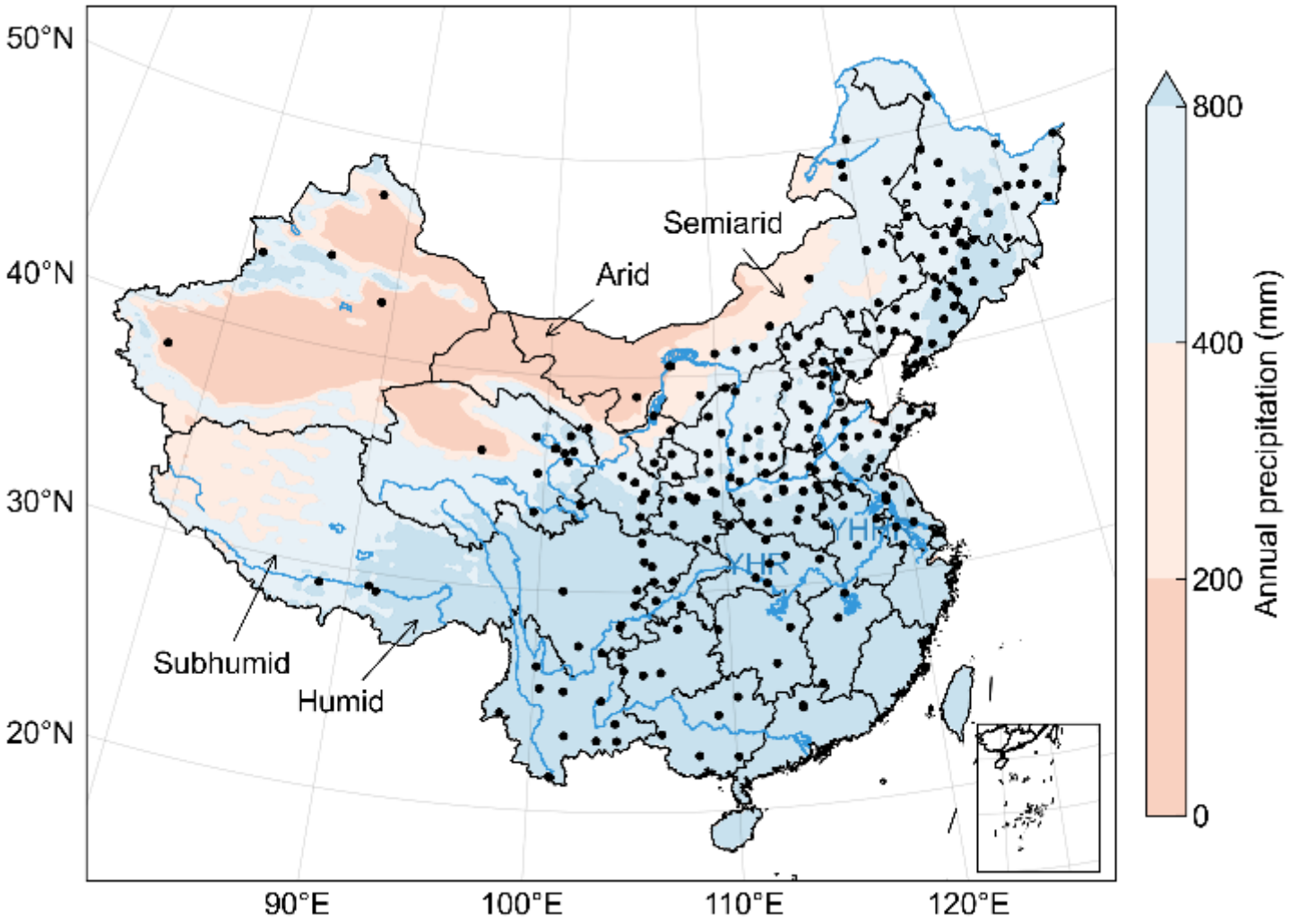

Figure 1

Spatial distribution of 245 first-order agrometeorological observation sites (dots) with arid, semiarid, subhumid, and humid climate zones according to annual precipitation total (units: mm). YHR and YHHR present the Yangtze-Han River and Yangtze-Huaihe River basins, respectively

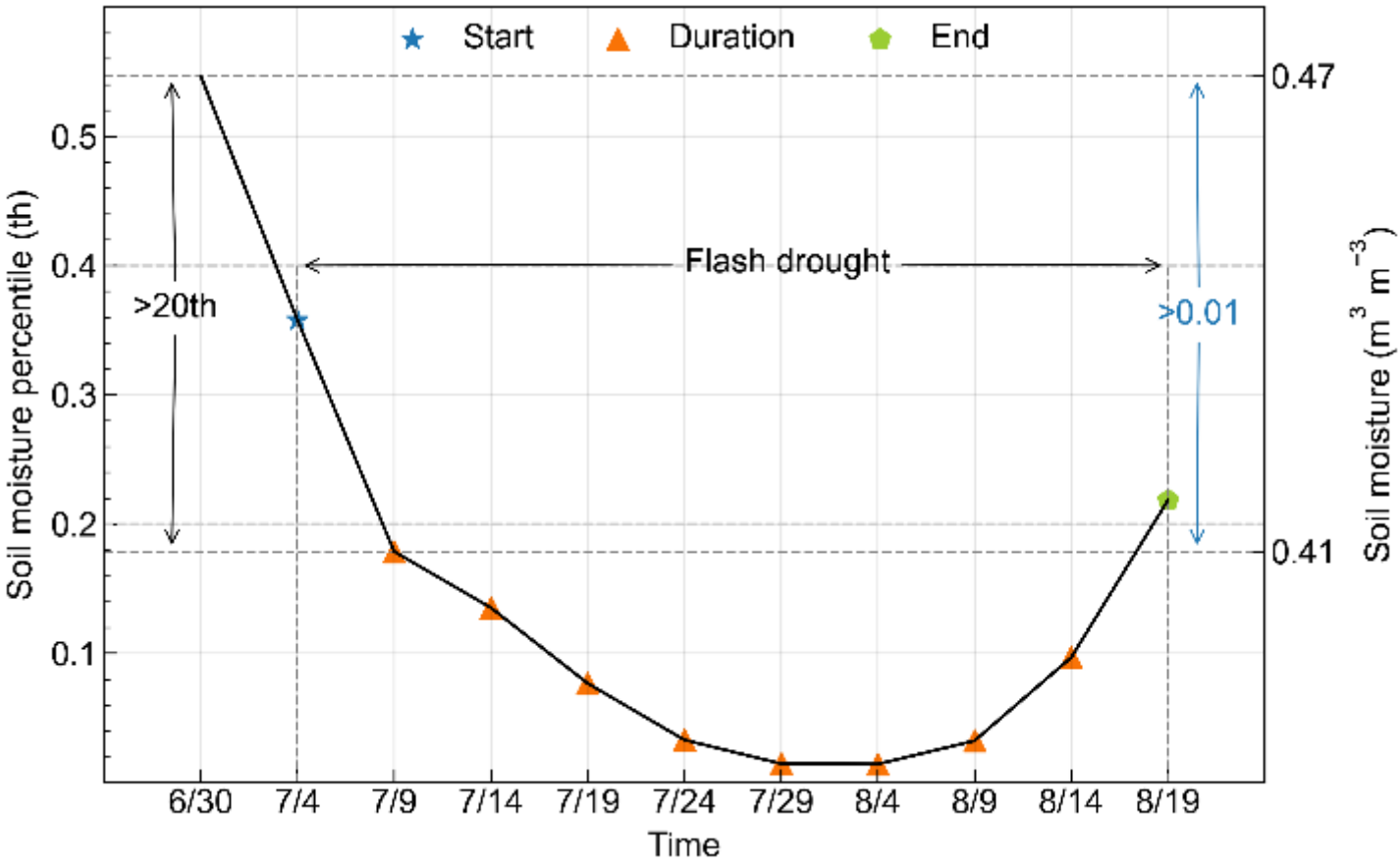

Figure 2

Schematic diagram for a flash drought event. The solid black line presents the pentad mean soil moisture percentile on a grid point (25°N, 112°E) during the 2007 flash drought. The first point less than 40th (asterisk), the first point greater than 20th (pentagonal), and the points between the two (triangles) indicate the onset, end, and duration of the flash drought event, respectively

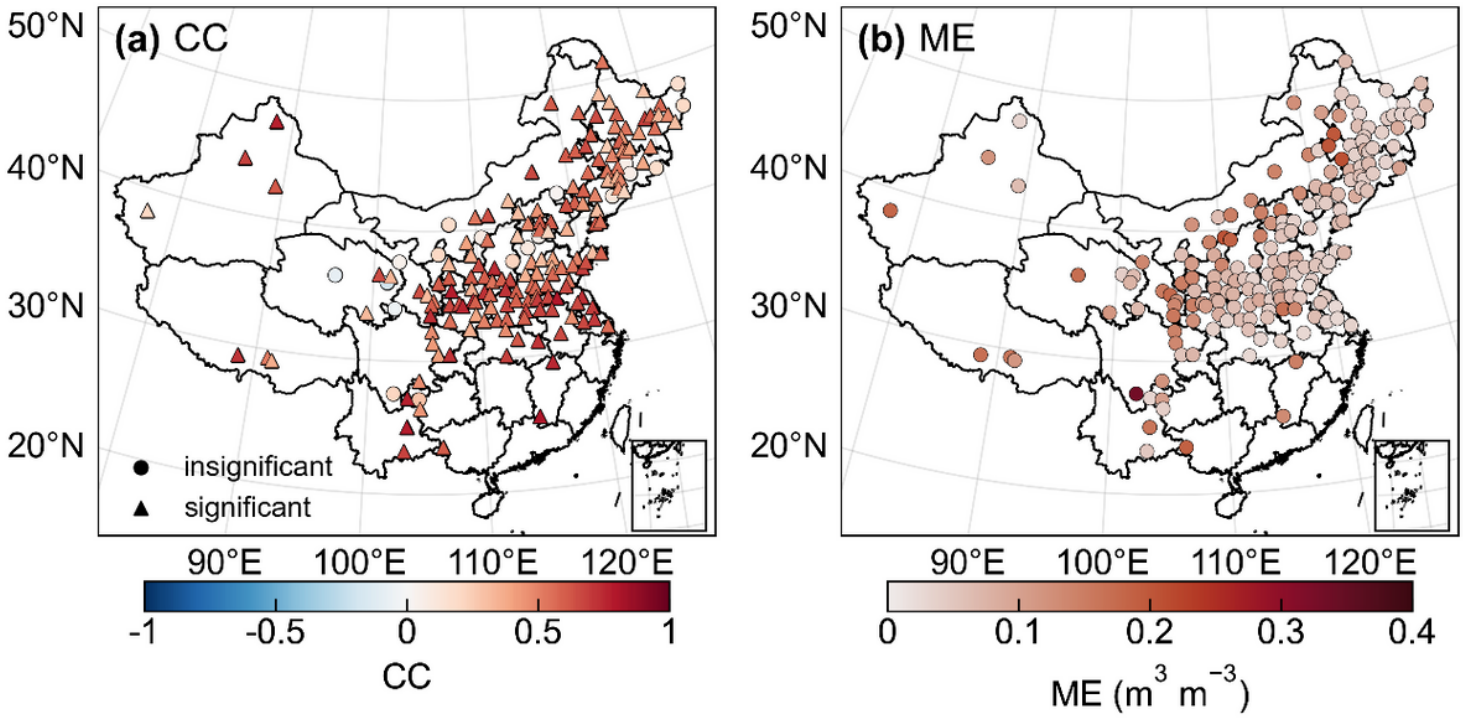

Figure 3

Spatial distribution of the correlation coefficients (CC, $p < 0.01$, circles indicate insignificant sites, and triangles indicate significant sites) and mean absolute errors (ME, units: $m^3\ m^{-3}$) between observations and ERA5-Land reanalysis soil moisture data in China from 1996 to 2010

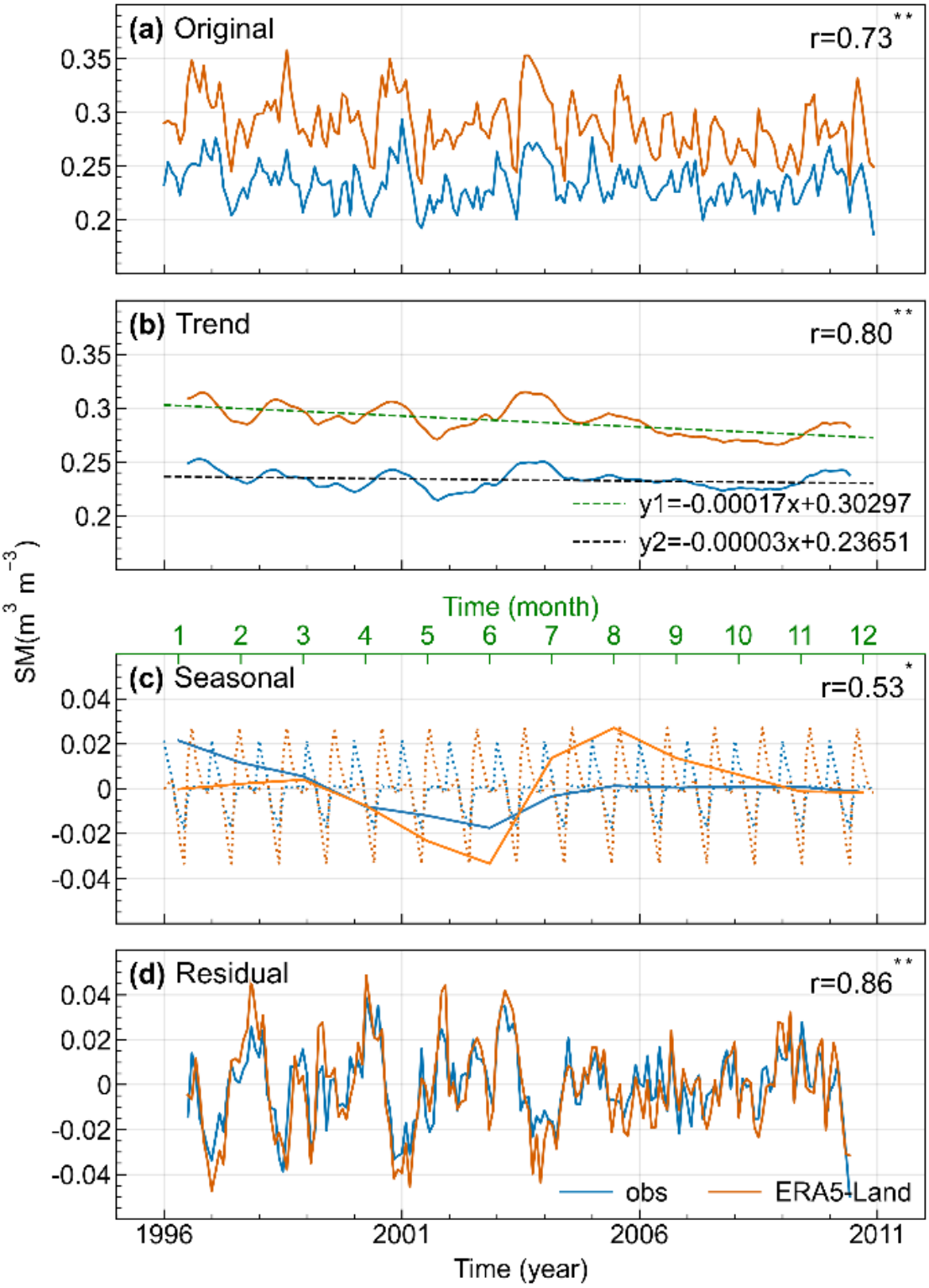

Figure 4

Seasonal decomposition analysis of monthly soil moisture time series resulted from observations and ERA5-Land reanalysis data during 1996-2010, *and ** denote significances at $p < 0.05$ and 0.01 levels

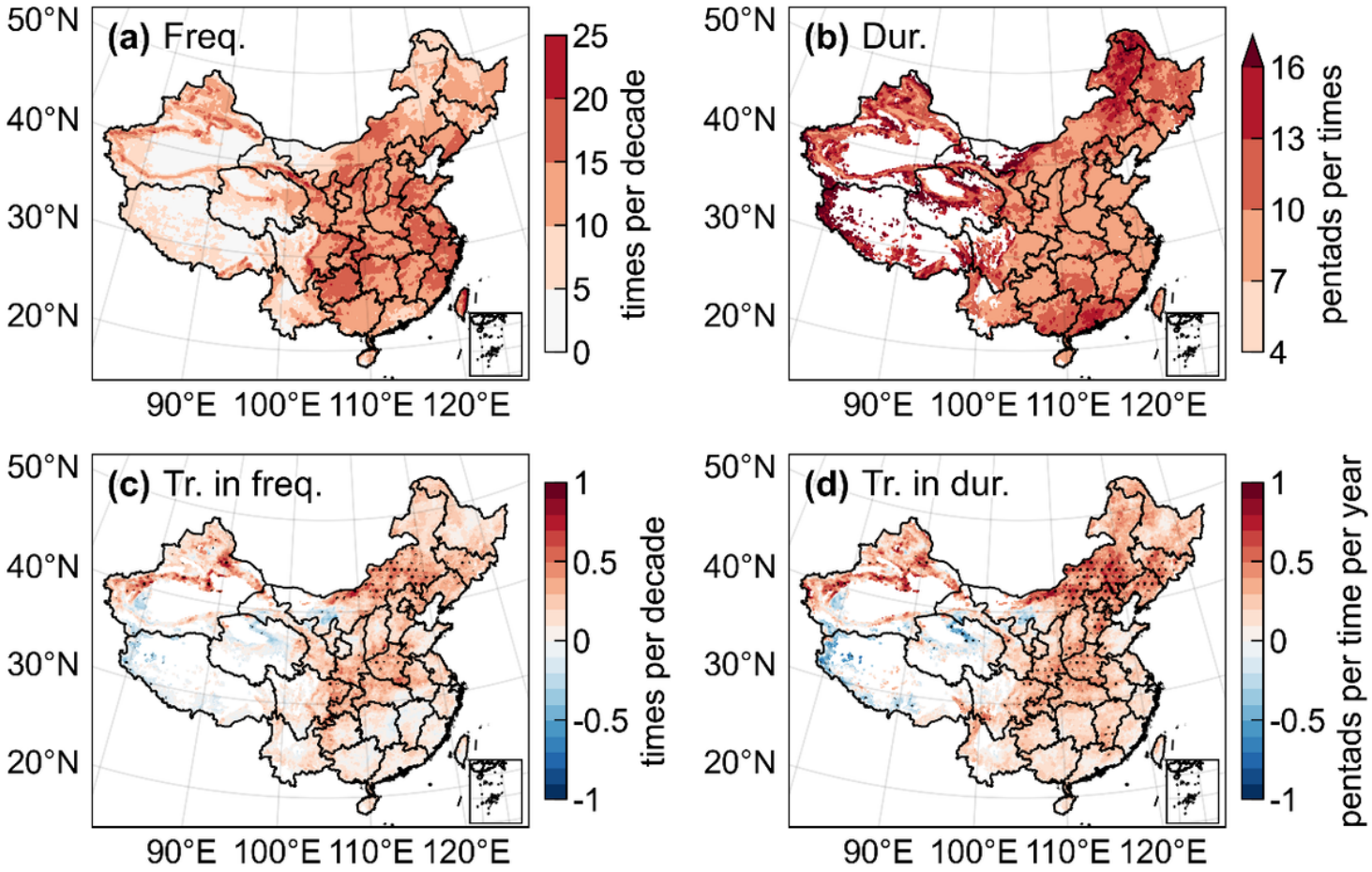

Figure 5

Spatial distribution of the frequencies (a, units: times per decade), mean durations (b, units: pentads per time), and trends of the two characteristic variables (c, d, $p < 0.01$, units: times per decade, pentads per time per year) of flash droughts in China from 1981 to 2021. Areas with less than 5 events per decade were excluded

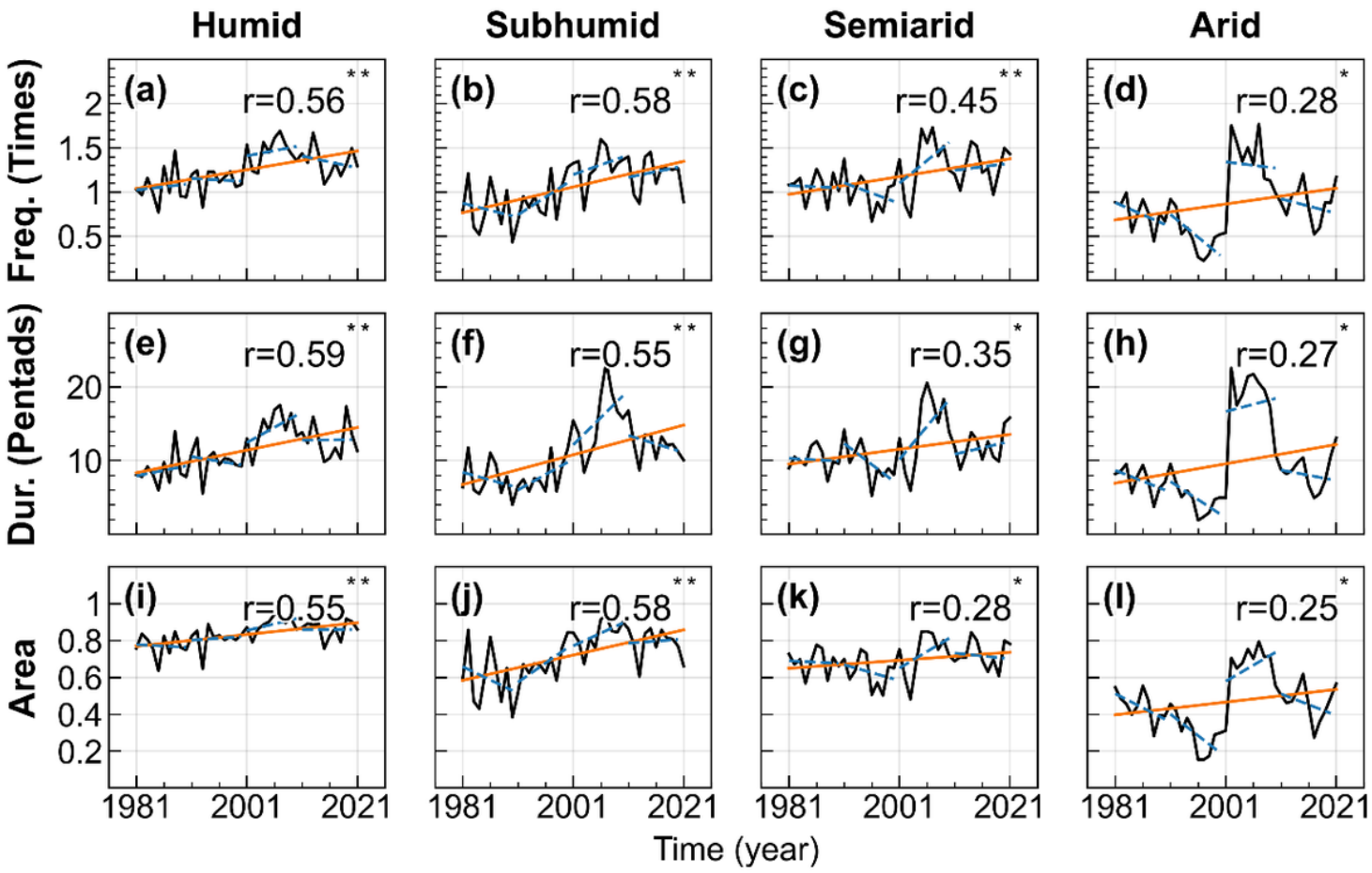

Figure 6

Interannual changes of flash drought frequencies (a-d, units: times), total durations (e-h, units: pentads), and affected areas (i-l) across climate zones from 1981 to 2021 and the linear trends were regressed using the least squares method on decadal (blue dashed lines) and 41-year (orange solid lines) time windows

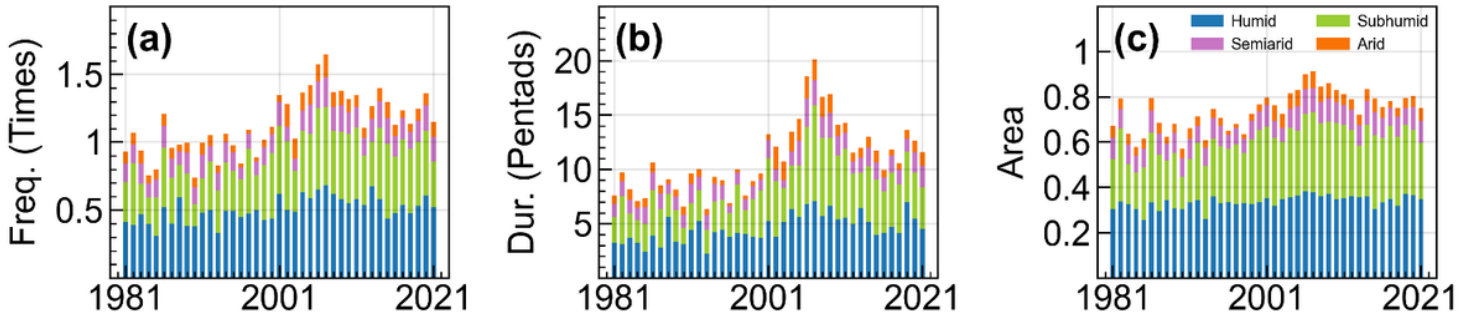

Figure 7

Histograms of flash drought frequencies (units: times), total durations (units: pentads), and affected areas of four climate zones in China from 1981 to 2021

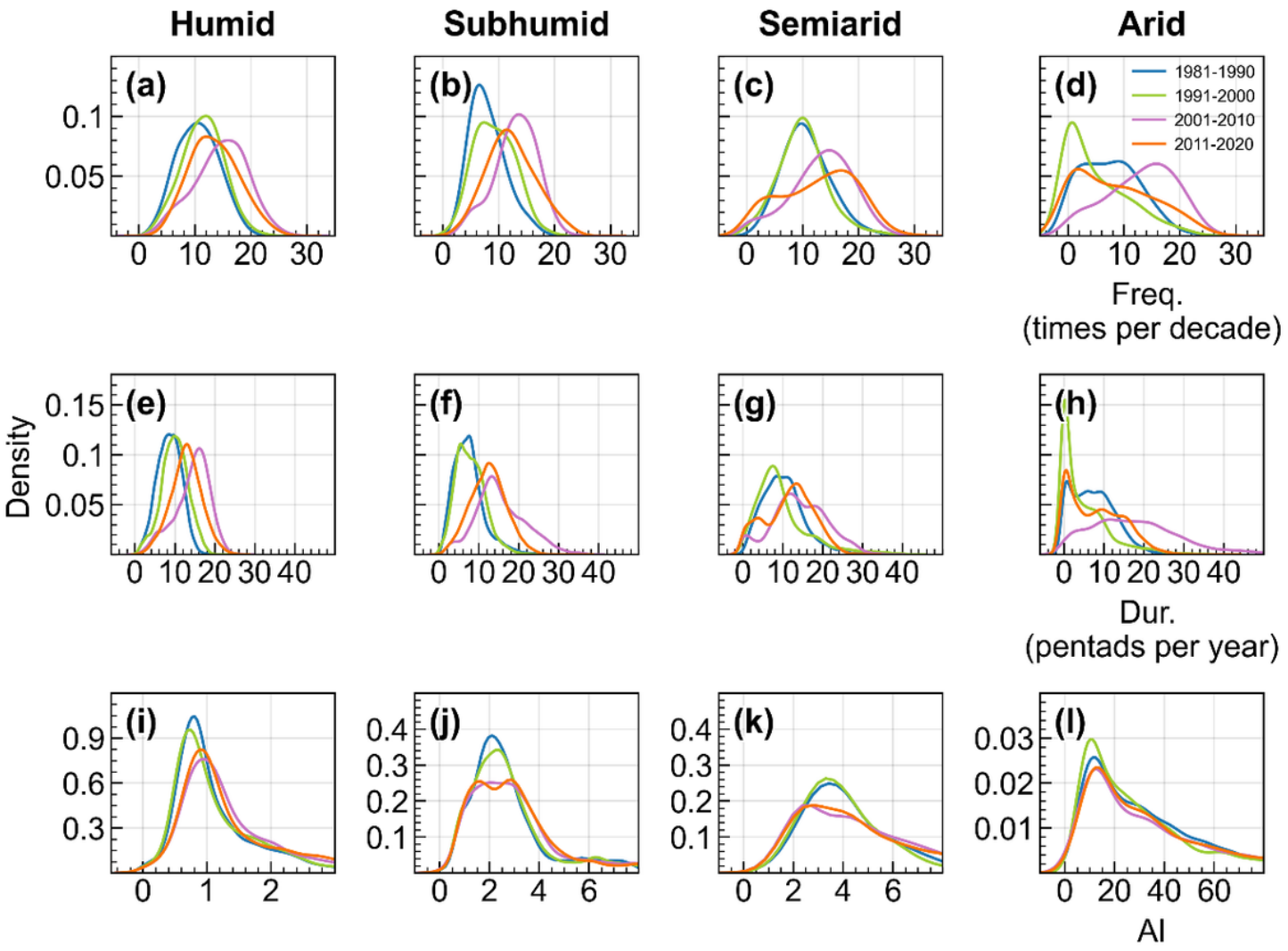

Figure 8

Probability distribution of the frequencies (unit: times per decade), total durations (unit: pentads per year), and AI indices of flash droughts in four climate zones in China from 1981 to 2020, and the frequencies and durations were accumulated on a monthly scale

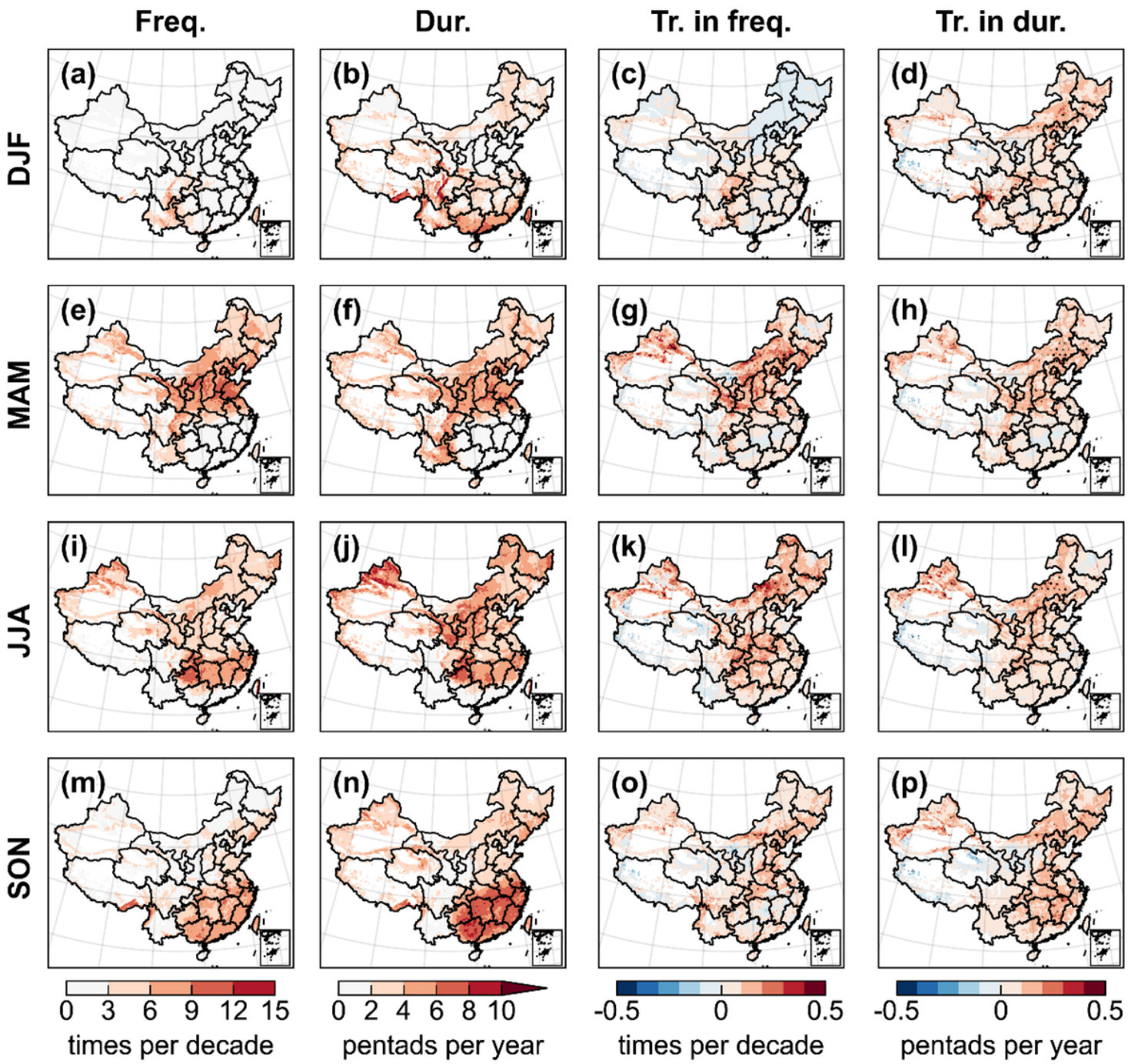

Figure 9

Spatial distribution of seasonal changes in the frequencies (unit: times per decade), total durations (unit: pentads per year), and their trends ($p < 0.01$, unit: times per decade, pentads per year) for flash droughts in China from 1981 to 2021

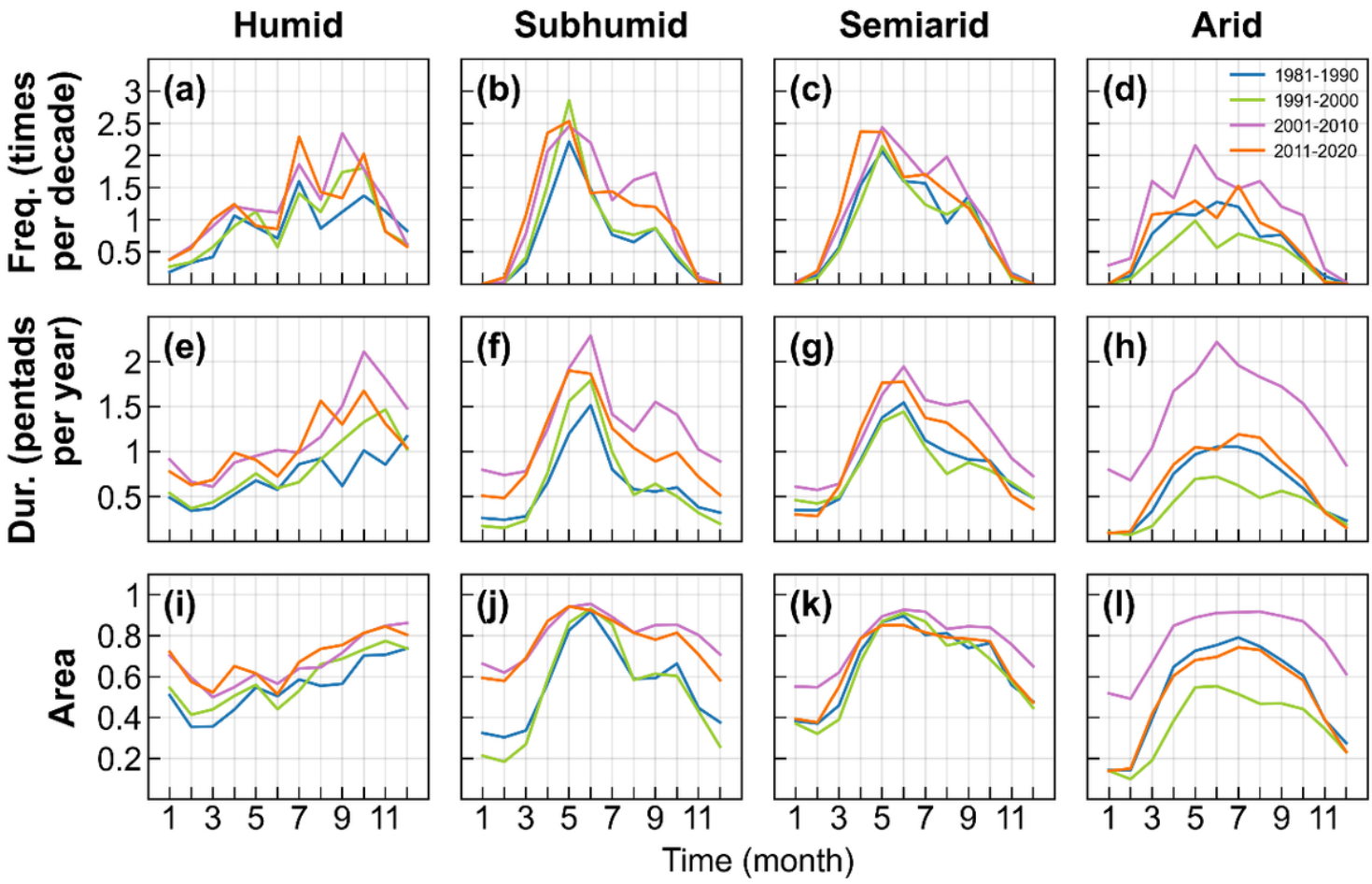

Figure 10

Monthly changes in the frequencies (unit: times per decade), total durations (unit: pentads per year), and affected areas of flash droughts in four climate zones in China from 1981 to 2020

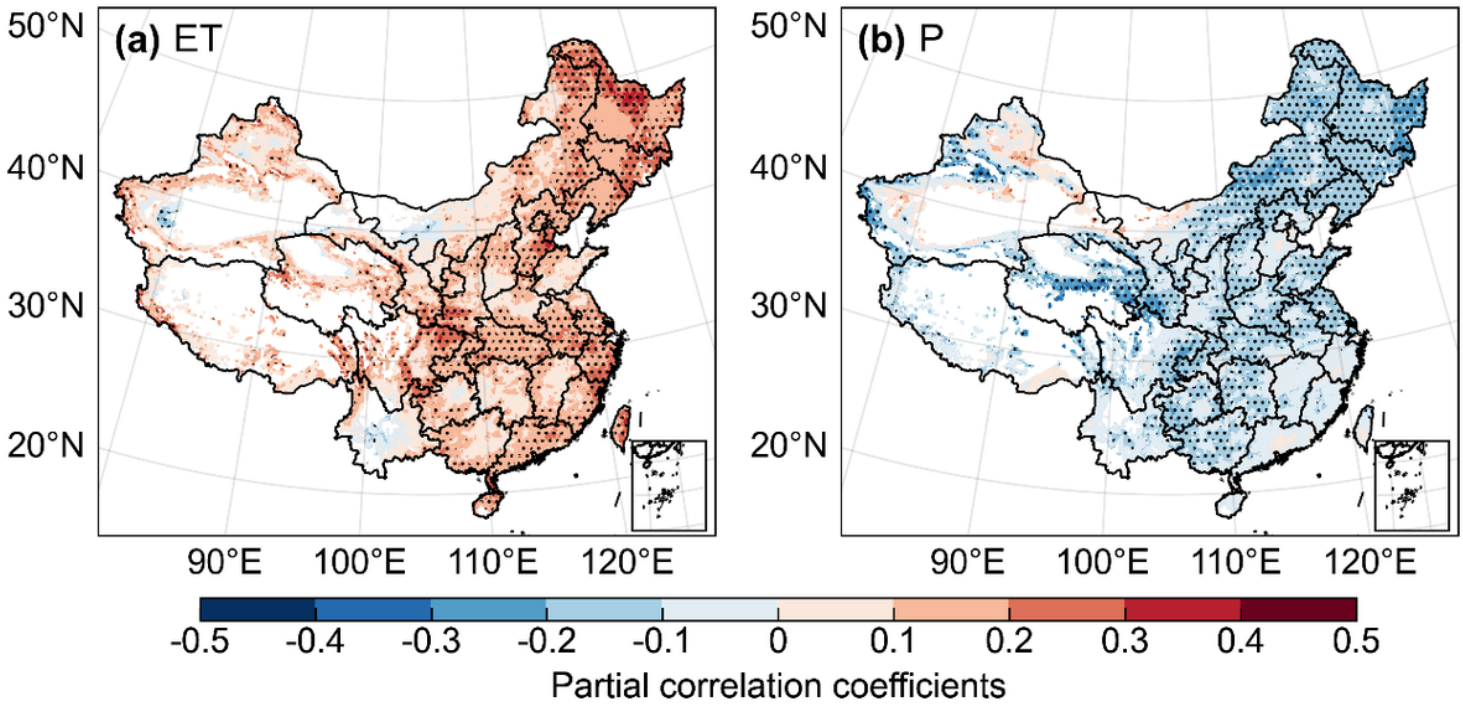

Figure 11

Spatial distribution of partial correlation coefficients between frequencies of flash droughts and evapotranspiration anomalies (a), and precipitation anomalies (b) in China from 1981 to 2021. Dots present significance at the $p < 0.01$ level

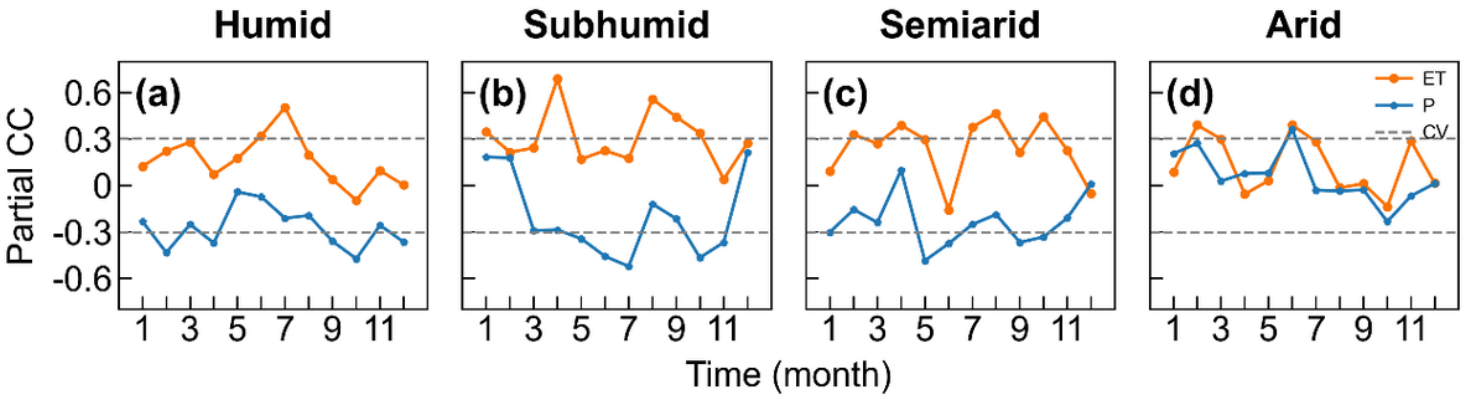

Figure 12

Monthly changes of the partial correlation coefficients between the frequencies of flash droughts and the anomalies of evapotranspiration and precipitation in four climate zones in China from 1981 to 2021. The dashed lines indicate critical values (CV) for significance at the $p < 0.05$ level

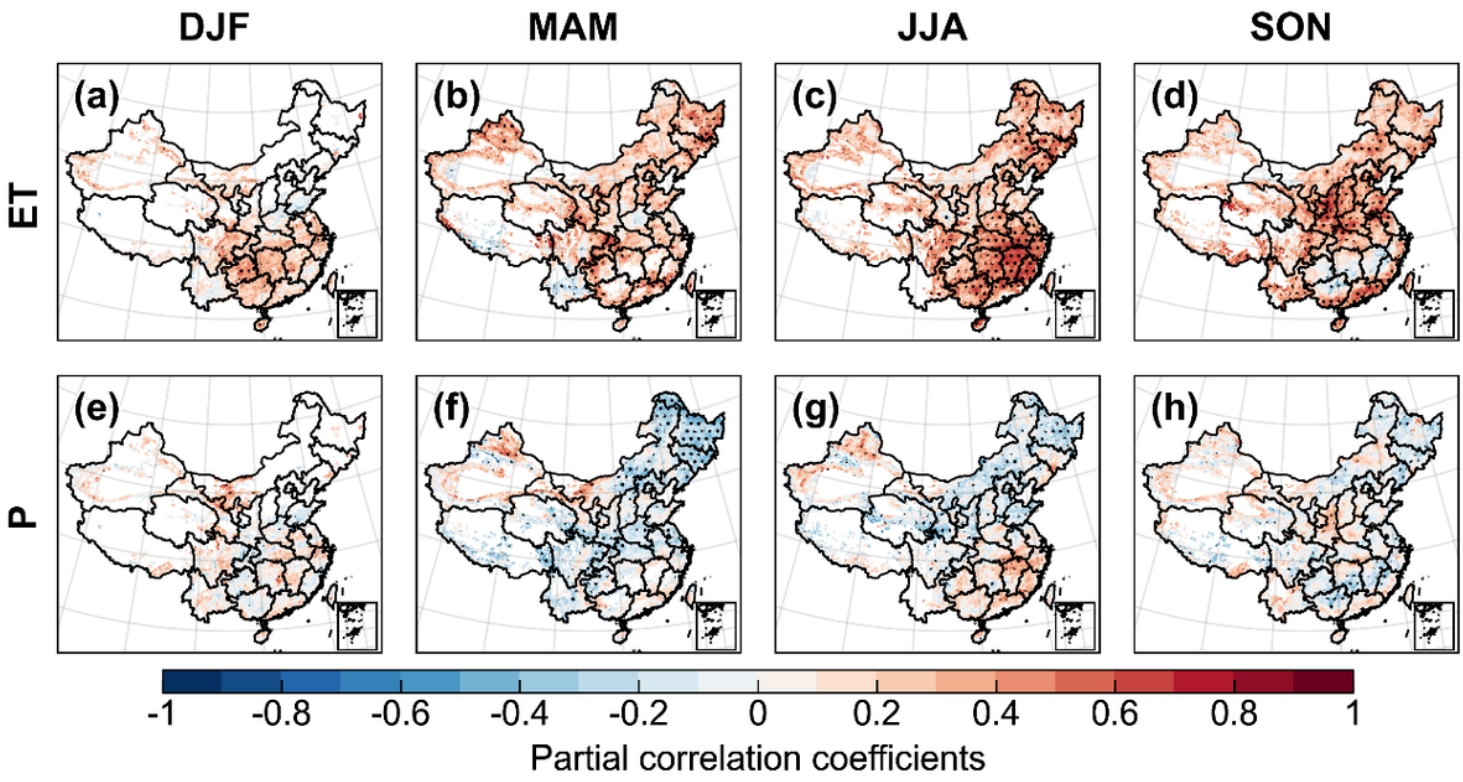

Figure 13

Spatial distribution of seasonal changes in partial correlation coefficients (p< 0.05) between frequencies of flash droughts and evapotranspiration (a-d) and precipitation (e-h) anomalies in China from 1981 to 2021. Dots present significance at the p< 0.01 level

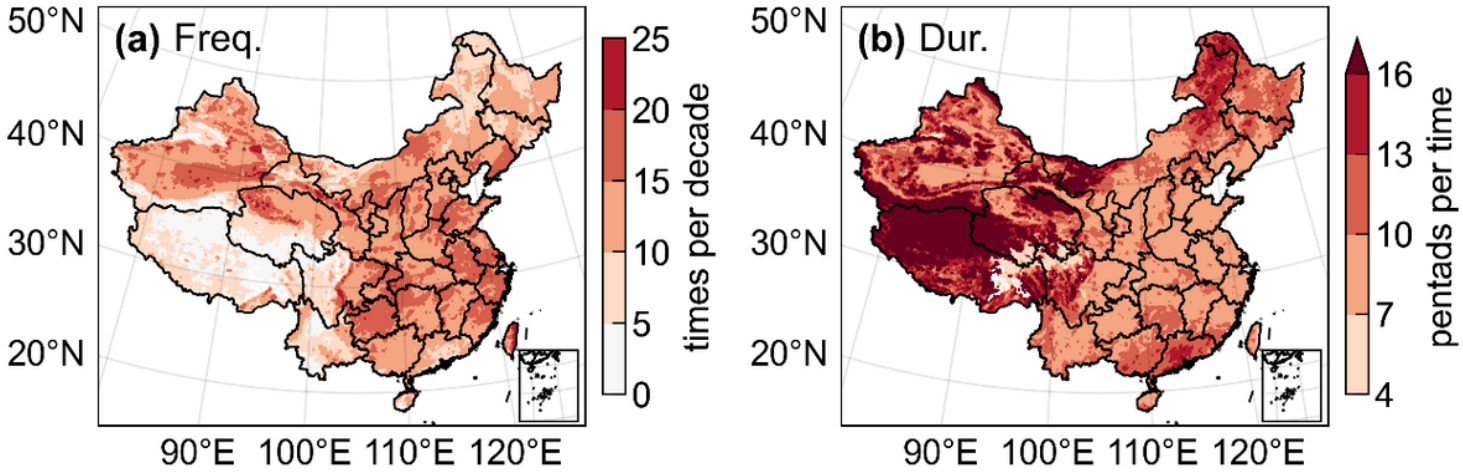

Figure 14

The same as Fig.9a, b, but under the definition without considering the criterion of absolute soil moisture variations (>0.01 m^3 m^{-3})